# A scanning nonlinear dielectric microscopic investigation of potential-induced degradation in monocrystalline silicon solar cells



doi: 10.1063/5.0004091

Applied Physics Letters

# A scanning nonlinear dielectric microscopic investigation of potential-induced degradation in monocrystalline silicon solar cells

Cite as: Appl. Phys. Lett. **116**, 182107 (2020); https://doi.org/10.1063/5.0004091
Submitted: 10 February 2020 . Accepted: 25 April 2020 . Published Online: 06 May 2020

Yasuo Cho, Sachiko Jonai, and Atsushi Masuda

Applied Physics Letters ARTICLE scitation.org/journal/apl

# A scanning nonlinear dielectric microscopic investigation of potential-induced degradation in monocrystalline silicon solar cells

Cite as: Appl. Phys. Lett. **116**, 182107 (2020); doi: 10.1063/5.0004091
Submitted: 10 February 2020 · Accepted: 25 April 2020 ·
Published Online: 6 May 2020



Yasuo Cho,[1,a)] Sachiko Jonai,[2] and Atsushi Masuda[2]

## AFFILIATIONS

[1]Research Institute of Electrical Communication, Tohoku University, 2-1-1 Katahira, Aoba-ku, Sendai 980-8577, Japan
[2]National Institute of Advanced Industrial Science and Technology, 1-1-1 Umezono, Tsukuba, Ibaraki 305-8568, Japan

[a)]**Author to whom correspondence should be addressed:** yasuocho@riec.tohoku.ac.jp

## ABSTRACT

Carrier distributions in monocrystalline silicon solar cells affected by potential-induced degradation (PID) were investigated using scanning nonlinear dielectric microscopy (SNDM), employing three samples with different PID levels. These observations clearly demonstrated that reductions in the carrier density were correlated with the extent of PID. Depth profile measurements showed that the solar cells were affected by PID to a significant depth of approximately 90 $\mu$m, equal to almost half the cell thickness. This result suggests that the $Na^+$ migration is readily induced by the application of a high voltage. Super-higher-order-SNDM was also employed to obtain a more precise analysis of the depletion layer distributions in monocrystalline silicon solar cells with and without the application of a high voltage. The data showed that the depletion layer of a sample without PID was thinner than that of a sample exhibiting PID, indicating that the carrier concentration in the former sample was higher. This finding was in good agreement with the results produced by direct quantitative dopant measurements using SNDM.



Crystalline silicon (Si) solar cells currently occupy an important place in the solar cell market. However, the potential-induced degradation (PID) of crystalline Si photovoltaic (PV) modules has recently been observed in large systems comprising significant numbers of PV modules. In these PV systems, numerous such modules are interconnected in series, such that the potential stress is imparted to some of the modules with consequently high power losses. PID in Si PV modules based on p-type crystalline Si solar cells had been previously investigated in detail.[1–5]

About the estimated changes in a solar cell during PID, for example, it has been reported that, due to the penetration of Na into the solar cell, a deep level is formed in the depletion layer or the base layer (p layer) and, as a result, carrier recombination through the level occurs.[4] Na is known to create a level in Si at a position 0.35 eV from the valence band. It has also been suggested that the current shunt path is formed by the intrusion of Na into stacking faults penetrating the pn junction (or that Na invading Si forms stacking faults).[5]

Even so, there is still a lack of understanding of the PID mechanism in solar cells, and obtaining more information regarding this phenomenon will require the measurements of carrier distributions on a microscopic scale. One of the authors previously succeeded in quantitatively analyzing such distributions in monocrystalline Si solar cells using scanning nonlinear dielectric microscopy (SNDM).[6,7] In the present study, the microscopic carrier distributions in monocrystalline Si solar cells exhibiting PID were investigated using this same technique. In addition, an enhanced version of this technique, referred to as the super-higher-order (SHO)-SNDM, was employed to visualize depletion layer distributions in such cells both with and without PID.

In SNDM, the sensor comprises a high-frequency inductance/capacitance ($LC$) self-oscillator that responds to changes in the capacitance [$\Delta C_{ts}(t)$] between a sample and a microscopy tip that is itself conductive, relative to a static capacitance ($C_{ts}$).[8] The capacitance between the sample and the tip represents a parallel capacitance relative to the $LC$ tank circuit. Consequently, the oscillation frequency [$\Delta f(t)$] varies from the initial value ($f_0$) as a consequence of $\Delta C_{ts}(t)$, and frequency modulation (FM) can be achieved via the application of a sinusoidal voltage to the sample. An FM demodulator subsequently demodulates the $\Delta f(t)$ signal, and data that are proportional to the change in capacitance with respect to voltage (that is, a $dC/dV$ signal) are obtained via a lock-in amplifier.

In the case that the sample is a semiconductor, the d$C$/d$V$ output is primarily determined by the capacitance of the depletion layer that exists underneath the tip.[9] The contact between the sample and the tip generates a localized metal–insulator–semiconductor (MIS) arrangement comprising the tip, an insulating layer, and the sample. The central insulating segment is frequently composed of a naturally occurring oxide phase. The change in the capacitance of the depletion layer for a typical MIS configuration is plotted against the applied voltage to the sample to produce a capacitance–voltage ($C$–$V$) graph. Because the d$C$/d$V$ data are correlated with the slope of this plot, this graph provides information concerning the dominant carrier concentration and polarity. Consequently, the spatial resolution of localized variations in these characteristics can be assessed. The application of a voltage to the sample relative to the grounded tip will generate a positive polarity d$C$/d$V$ output in the case of p-type carriers, while a negative signal will result from n-type carriers. In addition, the signal intensity will also vary with the dominant carrier concentration, although not in a linear manner.[6,10] It is common to combine the standard atomic force microscopy (AFM) with SNDM to adequately tune the force applied between the sample and the tip. This modification permits the d$C$/d$V$ data to be generated concurrent with the topographic images.

Figure 1 presents a schematic showing the experimental setup used to perform the PID testing of p-type monocrystalline Si solar cells in this study. Three such cell samples were prepared for these trials, comprising a non-PID sample (sample 1) and two units that had been degraded by applying −2000 V at 65 °C for approximately 1.5 h (sample 2) and 10 h (sample 3). These two units exhibited mild (sample 2) and heavy (sample 3) degrees of PID. Each cell was cross-sectioned, after which the cross section was polished chemomechanically and assessed using SNDM. The resulting images are provided in Fig. 2, which clearly demonstrate that the image contrast was reduced as the degree of PID was increased.

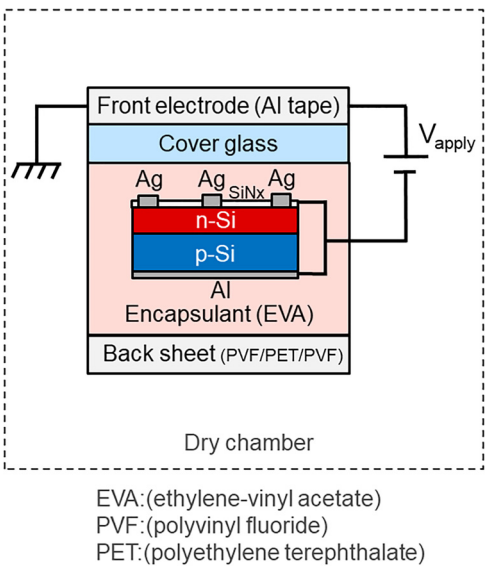


**FIG. 1.** A schematic diagram of the PID testing of a p-type c-Si standard PV module.

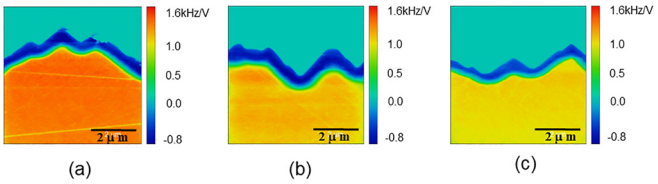


**FIG. 2.** SNDM images of the cross sections of monocrystalline Si solar cell samples (a) without PID (sample 1), (b) with mild PID (sample 2), and (c) with heavy PID (sample 3). The polarity of the SNDM signal corresponds to the carrier polarity.

To permit a quantitative comparison of the carrier concentrations in samples 1 and 3, both p-type and n-type standard Si staircase samples were prepared for the calibration of the carrier densities.[6] These samples had seven and six layers, respectively, each with a different carrier density. The carrier density in each layer was determined using secondary ion mass spectrometry (SIMS), and these values ranged from $1 \times 10^{16}$ to $1 \times 10^{20}$ cm$^{-3}$. These standard samples were polished at the same time as the Si solar cell test samples and so it was assumed that the P (phosphorous)-diffused Si solar cells and the standard samples had the same surface characteristics. The standard samples were assessed after the SNDM analyses of the P-diffused Si solar cells.

Using the data obtained from the standard samples, we calibrated the SNDM signal to obtain the quantitative values for the carrier densities. Figure 3 shows the two-dimensional SNDM images (that is, the raw data) and one-dimensional carrier density profiles along the white lines in the SNDM images for both a non-PID sample (sample 1) and a heavy PID sample (sample 3). The magnitude of the SNDM signal changes with the carrier density and, in the case of the non-PID sample (sample 1), the electron density decreases exponentially on going from the surface to the bulk. In contrast, the electron density in the heavy PID sample (sample 3) is much lower than that in the non-PID sample and does not decrease exponentially from the surface to the bulk. This result indicates that the carrier concentration is reduced by several orders of magnitude due to the effect of PID. Moreover, in the depletion layer, the tip–sample capacitance ($C_{ts}$) value is affected by

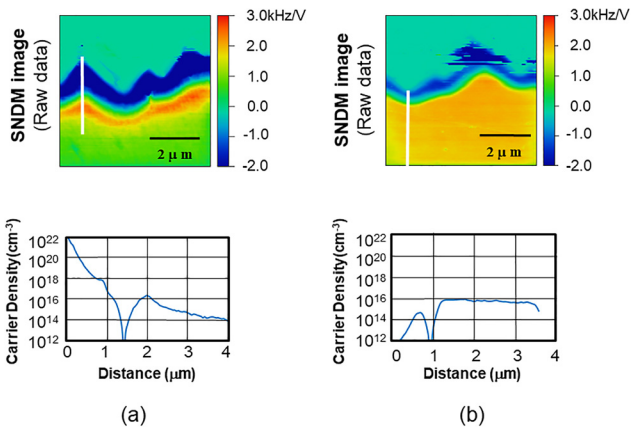


**FIG. 3.** Two-dimensional SNDM images (that is, raw data) and one-dimensional carrier density profiles along the white lines in the SNDM images of (a) a non-PID sample (sample 1) and (b) a heavy PID sample (sample 3).

both the p- and n-type layers. Therefore, it should be noted that the calibrated results with the values of less than approximately $1 \times 10^{15}$ cm$^{-3}$ in Fig. 3 may not be correct.

We subsequently performed depth profile measurements to determine the depth to which the solar cells are affected by PID. The data acquired from sample 1 (non-PID sample) and sample 2 (the mild PID sample) are provided in Fig. 4 (it should also be noted that sample 3 gave almost the same results as sample 2). Surprisingly, the data demonstrate that the Si solar cell with PID was affected to a very significant depth of approximately 90 $\mu$m from the textured surface. This suggests that the $Na^+$ (sodium cation) migration from the surface proceeds very easily upon applying a high voltage. Unfortunately, based solely on the results obtained in this study and knowledge from the previously reported literatures, it is difficult to clarify the mechanism for this significant depth being affected by PID. To make it clear, further investigation is needed. However, we believe that this finding will be useful in providing knowledge for further investigation of the cause of PID by informing experts in this field that solar cells are deeply affected by PID.

A new method related to SNDM has recently been developed that returns both a d$C$/d$V$ signal and higher-order differential values. This technique provides data regarding various materials that are significantly more precise and is referred to as SHO-SNDM.[12] $\Delta C$–$V$ plots at individual pixels can be readily reconstructed using SHO-SNDM, such that the analytical power of the method is greatly increased. SHO-SNDM employs an equivalent experimental apparatus to SNDM other than the incorporation of a multi-channel lock-in amplifier. During analyses using this technique, higher harmonic components are detected. This is in contrast to the standard SNDM, which employs solely the first-order d$C$/d$V$ harmonic component. In this method, $\Delta f(t)$ is correlated with $\Delta C_{ts}(t)$, which in turn varies according to the ac voltage that is applied between the sample and the tip: $V(t) = V_p \cos \omega_P$. The correlation between $\Delta f(t)$ and $\Delta C_s$ $(t)$ can be summarized as

$$\Delta f(t) \propto -\Delta C_{ts}(t) = \sum_{n=1}^{\infty} (\Delta C_n^{\cos} \cos n\omega_p t + \Delta C_n^{\sin} \sin n\omega_p t), \quad (1)$$

where both $\Delta C_n^{\cos}$ and $\Delta C_n^{\sin}$ represent the Fourier coefficients. Both terms can be determined via the extraction of the nth order $\Delta C_{ts}(t)$ harmonic components that are correlated with the demodulated FM signal generated by the SNDM probe. The $\Delta C$–$V$ plot can be obtained from $\Delta C_{ts}(t)$ data (generated using $\Delta C_n^{\cos}$ and $\Delta C_n^{\sin}$) and $V(t)$ values (using time, $t$, as a parameter).[12] The use of higher-order differential terms is the same as working with the Fourier series expansion harmonics, meaning that the SHO-SNDM technique is especially applicable to the analysis of semiconductors.

Based on the $\Delta C$–$V$ curve shape after reconstruction, the distribution of the depletion layer can be assessed. The $\Delta C$–$V$ plot is generated by producing a plot of $\Delta C_{st}(t)$ as a function of $V(t)$ along the $V$–$\Delta C_{ts}$ plane for $t$ over the range of $(-\pi/\omega_p, +\pi/\omega_p)$. Curves exhibiting linear increases and decreases are produced in the case that the tip is in contact with the p- and n-type regions, respectively. If the tip is in

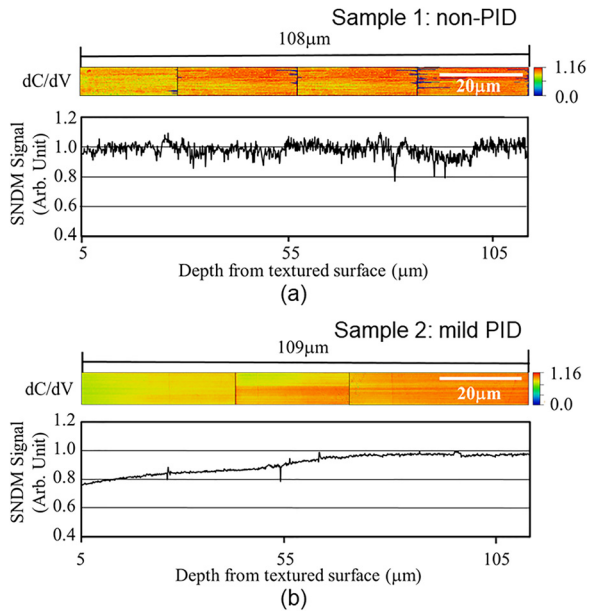


**FIG. 4.** Depth profiles of the SNDM signals (a) for sample 1 (non-PID sample) and (b) for sample 2 (mild PID sample). This Si solar sell with PID was evidently affected by PID to a depth of 90 $\mu$m.

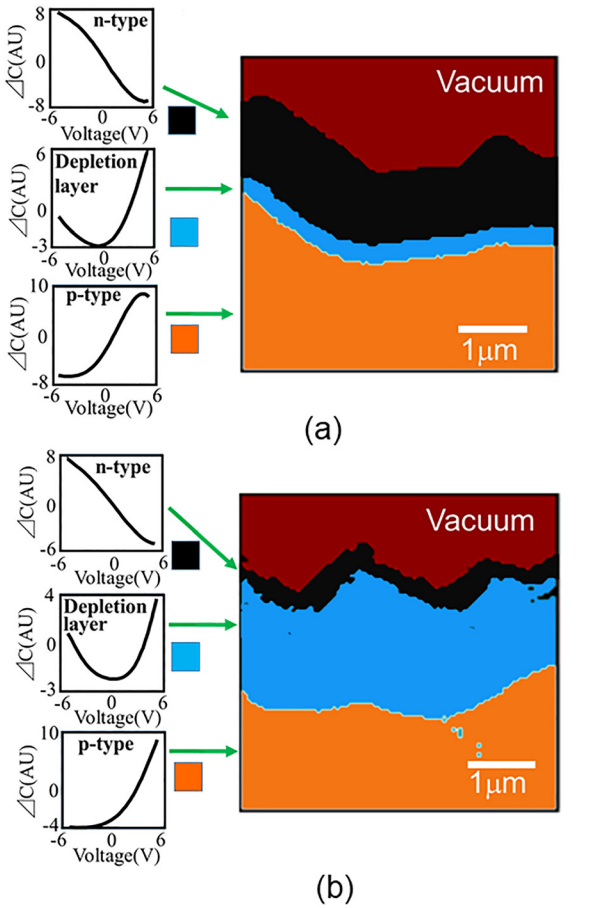


**FIG. 5.** SHO-SNDM images of (a) a non-PID sample (sample 1) and (b) a heavy PID sample (sample 3).

contact with the depletion layer, the curve describes a V shape because the capacitance below the tip will depend on whether the carriers are p- or n-type. In this scenario, a negative bias, $V$, will mean that electrons approach the tip from the n-type area such that $C_{ts}$ is increased. However, if $V$ is positive, $C_{ts}$ will become greater as well because holes will migrate to the tip from the p-type area. These effects produce a characteristic V-shaped plot[11,12] that reflects the contributions of both the n-type and the p-type zones to the capacitance between the sample and the tip.

This study also examined the distribution of the depletion layer thickness along the cross sections of monocrystalline Si solar cells with and without PID, using SHO-SNDM.[12] In these trials, the harmonic components of the capacitance variation up to the sixth harmonic were examined and $\Delta C$–$V$ curves were reconstructed from the SHO-SNDM data. We categorized each pixel as either the n-type, depletion layer or the p-type, based on the shape of the $\Delta C$–$V$ curve. That is, a monotonic decrease indicates n-type, a V-shaped curve indicates a depletion layer, and a monotonic increase demonstrates p-type. The results are shown in Fig. 5 together with the typical $\Delta C$–$V$ curves. In the SHO-SNDM images, the black and orange areas indicate the n-type and p-type regions, respectively, while the blue areas indicate depletion layers. From these results, it is evident that the depletion layer of sample 1 was thinner in the convex areas than in the concave areas, suggesting that the carrier concentrations in the convex areas were higher. It is also apparent that the depletion layer in sample 1 was much thinner than that of sample 3. This result indicates that the carrier concentration in the non-PID sample was higher than that in the PID sample, in good agreement with the direct quantitative dopant data obtained using SNDM and is shown in Fig. 3.

In conclusion, this study examined the extent to which the carrier distributions in monocrystalline silicon solar cells were affected by PID using SNDM. Reductions in the carrier density in accordance with the extent of PID were clearly observed, and quantitative measurements demonstrated that the electron concentration was reduced by several orders of magnitude due to PID. Depth profile data showed that very deep regions relative to the textured surfaces of the solar cells were affected by PID, suggesting that the $Na^+$ migration proceeded easily upon the application of a high voltage. The SHO-SNDM technique was used to analyze depletion layer distributions in monocrystalline Si solar cells with and without PID. The data showed that the depletion layer of the non-PID sample was thinner than that of a PID sample, indicating that the carrier concentration in the former was greater. This work demonstrates that SNDM is a very useful means of investigating the PID effect through the measurement of carrier distributions in monocrystalline silicon solar cells.

This work was supported in part by a Grant-in-Aid for Scientific Research (No. 16H02330) from the Japan Society for the Promotion of Science. Funding was also obtained from the New Energy and Industrial Technology Development Organization.

## REFERENCES

[1]S. Jonai and A. Masuda, AIP Adv. **8**, 115311 (2018).
[2]J. Berghold, O. Frank, H. Hoehne, S. Pingel, B. Richardson, and M. Winkler, in Proceedings of the 25th European Photovoltaic Solar Energy Conference and Exhibition, Valencia, Spain (2010), p. 3753.
[3]P. Hacke, M. Kempe, K. Terwilliger, S. Glick, N. Call, S. Johnston, S. Kurtz, I. Bennett, and M. Kloos, in Proceedings of the 25th European Photovoltaic Solar Energy Conference and Exhibition, Valencia, Spain (2010), p. 3760.
[4]W. Luo, Y. Sheng Khoo, P. Hacke, V. Naumann, D. Lausch, S. P. Harvey, J. Prakash Singh, J. Chai, Y. Wang, A. G. Aberle, and S. Ramakrishna, Energy Environ. Sci. **10**, 43 (2017).
[5]V. Naumann, D. Lausch, A. Hähnel, J. Bauer, O. Breitenstein, A. Graff, M. Werner, S. Swatek, S. Großer, J. Bagdahn, and C. Hagendorf, Sol. Energy Mater. Sol. Cells **120**, 383 (2014).
[6]K. Hirose, K. Tanahashi, H. Takato, and Y. Cho, Appl. Phys. Lett. **111**, 032101 (2017).
[7]Y. Cho, A. Kirihara, and T. Saeki, Rev. Sci. Instrum. **67**, 2297 (1996).
[8]Y. Cho, S. Atsumi, and K. Nakamura, Jpn. J. Appl. Phys., Part 1 **36**, 3152 (1997).
[9]C. C. Williams, J. Slinkman, W. P. Hough, and H. K. Wickramasinghe, Appl. Phys. Lett. **55**, 1662 (1989).
[10]Y. Cho, Jpn. J. Appl. Phys., Part 1 **56**, 100101 (2017).
[11]H. Edwards, R. McGlothlin, R. San Martin, U. Elisa, M. Gribelyuk, R. Mahaffy, C. Ken Shih, R. Scott List, and V. A. Ukraintsev, Appl. Phys. Lett. **72**, 698 (1998).
[12]N. Chinone, T. Nakamura, and Y. Cho, J. Appl. Phys. **116**, 084509 (2014).